Cerâmica. 2024, v.70:ePDLQ5554 http://dx.doi.org/10.1590/PDLQ5554
ORIGINAL ARTICLE

Development of alumina-based ceramic microspheres as adsorbent for the removal of Zn^{2+}, Ni^{2+}, and Mn^{2+} ions in a fixed-bed column system

Tatiana Martinez Moreira, Luis Antonio Genova
University of São Paulo - Institute of Energy and Nuclear Research - Center for Materials Science and Technology
Avenida Professor Lineu Prestes, 2242 - Brazil - São Paulo - SP - CEP 05508-000

Abstract

Heavy metals are among the most harmful pollutants to the environment and human health. They are present in various industrial processes, requiring increasingly efficient treatments for removing their excessive concentration at acceptable levels before disposal. Adsorption is a widely used technique due to its efficiency, selectivity, and low cost. In this work, alumina ceramic microspheres, both pure and Si-doped, were produced by internal gelation to serve as adsorbents in the treatment of aqueous effluents containing Zn²+, Ni²+, and Mn²+, originating from the tri-cationic phosphatization process in the automotive industry. These microspheres, calcined at 600 °C and 700 °C, were characterized according to size distribution, specific surface area, gas adsorption, XRD, SEM, and optical microscopy. The effluent was treated in a fixed-bed column filled with these microspheres. The concentration of the three heavy metals was reduced by more than 90%, indicating the high efficiency of alumina ceramic microspheres as adsorbents of these heavy metals.
Keywords: Adsorption, heavy metals, fixed-bed column, alumina ceramic microspheres, internal gelation.

INTRODUCTION

Phosphatization processes are widely used in industry as a surface treatment for metals, especially thin ones, to improve adhesion between the metal surface and the paint layer, as well as to provide corrosion protection.[1-3] Tricationic phosphatization baths are the most commonly used for the formation of conversion layers in the automotive painting process and are also used in white line appliance painting systems. They are zinc, nickel, and manganese phosphates and they emerged with the need to improve the process. The presence of these elements in phosphatization systems leads to grain refinement in the conversion layer, significantly increasing the adhesion of the paint on the metallic substrate, which increases its resistance to corrosion [4-6].

This process, however, consumes a large amount of water, generating effluents with high concentrations of heavy metals, which can lead to environmental contamination and risks to human health, if improperly disposed. Thus, an efficient treatment of this wastewater is essential, aiming at reducing their concentration to levels allowed for discharge. To give a sense of the scale of the issue, in a car assembly plant with the production of 30 cars per hour, 2 to 2.5 m^3 of this effluent is produced per hour [7-9].

Among the different methods used for treating residual aqueous solutions containing heavy metals (ion exchange, electrocoagulation, reverse osmosis, chemical treatments, among others) [10-12]. The adsorption process stands out for its versatility, simplicity of operation, selectivity, efficiency, and cost-effectiveness. It is a mass transfer operation, in which certain solids can concentrate on their surface specific substances existing in liquid or gaseous fluids, enabling their separation [13-17].

Alumina (Al_2O_3) in the gamma phase is an adsorbent material of great interest due to its high specific surface area and strong capacity to adsorb both organic and inorganic compounds. Alumina can be produced in the form of porous ceramic microspheres, allowing its use in effluent treatment operations in column systems (fixed-beds). Its adsorption efficiency is related to its specific surface area, particle morphology, porosity, crystalline phase, and doping with various elements, among other physical and chemical properties [18-23].

Internal gelation is an effective and versatile method for producing porous alumina microspheres in large quantities, allowing for control over various characteristics and properties that can be modified or introduced during the manufacturing process. The microspheres also have the advantage of adapting very well to the effluent treatment process in fixed-bed columns, which enables the efficient treatment of large volumes of effluent [24-29].

This work aimed to produce porous alumina-based ceramic microspheres via internal gelation, characterizing them and evaluating their efficiency in retaining heavy metals through adsorption in a fixed-bed column. The study focused on an aqueous solution containing Zn², Ni², and Mn² in concentrations similar to those found in effluents from the tricationic phosphating process used in the automotive industry.

MATERIALS AND METHODS

Pure and doped (5 wt.% of Si) porous alumina microspheres were produced by the internal gelation method. A stock solution of metal ion was prepared by dissolving adequate amounts of aluminum nitrite ($Al(NO_2)_3$) into deionized water

* *tatiana.moreira@usp.br*
https://orcid.org/0000-0003-2540-010X

to obtain a metal concentration of 1.6 M. Stock solutions of hexamethylenetetramine (HMTA $C_6H_{12}N_4$) and urea ($CO(NH_2)_2$) was prepared by dissolving adequate amounts of these compounds into deionized water.

Broths solutions were obtained by mixing both stock solutions at 5 °C to prevent any premature gelation. The amount of HMTA and urea present in a broth was defined by the molar ratio of HMTA or urea on metal (R_x = [x]/[metal], where x is HMTA or urea). In this work were used R_{HMTA} = 1.6 and R_{urea} = 2.0. The prepared solution, kept at 5 °C, was dropped using a developed microfluidic device, in a double-jacketed column, containing soybean oil heated to 90 °C.

The dropping device allows the control and regularity of the size of the drops produced. The contact of the droplet with the oil causes its heating and the decomposition of HMTA into ammonia and formaldehyde. The ammonia hydrolyses the metallic ion, transforming the drop into a gelatinous sphere. Figure 1 shows the gelation column apparatus and a schematic diagram.

The oil temperature and the column height are important parameters of the process to allow the gelification of the microspheres, and these acquire adequate mechanical resistance on their way down the column, before reaching the lower reservoir.

After the process, the microspheres were washed, dried, and calcined at 600 °C and 700 °C for one hour, with a heating and cooling rate of 1 °C/minute. The characterization was performed using BET (specific surface area), BJH (gas adsorption), XRD (X-ray diffraction), SEM (Scanning Electron Microscopy), and optical microscopy techniques.

The solution containing heavy metals, used in this study, and simulating the effluent produced in the process of tricationic phosphatization in an automotive industry, has a typical concentration of 13.50 $mg.L^{-1}$ of Zn, 4.50 $mg.L^{-1}$ of Mn and 5.50 $mg.L^{-1}$ of Ni. The adsorption tests were carried out in a fixed-bed column system, using a peristaltic pump to control the flow rate of the solution to be treated at 10 ml/min in the used configuration of the test (Figure 2).

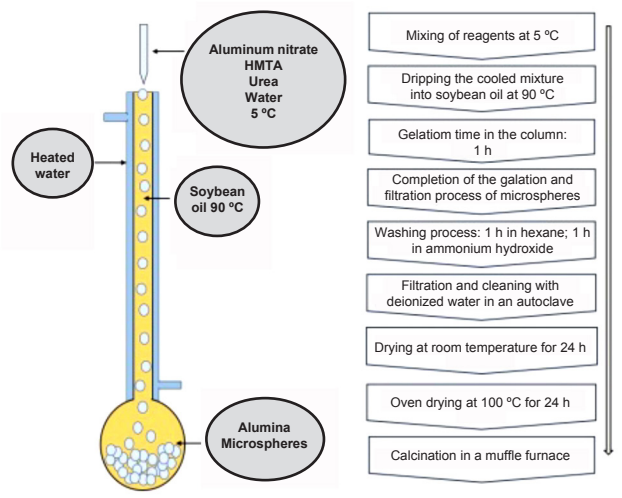

Figure 1: Internal gelation column for the production of alumina-based ceramic microspheres and a flowchart of the process steps.

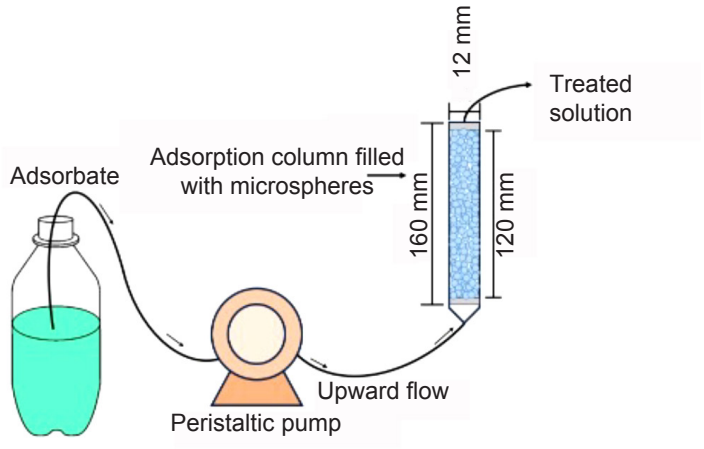

Figure 2: Schematic of a fixed-bed adsorption system, including the dimensions of the glass column used in the process.

The mass of microspheres to fill the column was around 6.5 g, with an average packing of 0.85 g/cm^3. During the test, samples of the treated solution were collected at different times, determining the concentration of heavy metals by inductively coupled plasma optical emission spectroscopy (ICP-OES), as well as its pH and electrical conductivity.

RESULTS AND DISCUSSION

Alumina-based ceramic microspheres

Figures 3(a) and 3(b) show a SEM image (Tabletop Microscope, TM 3000 Hitachi) of the alumina-based microspheres and figure 3(c) shows an optical microscopy image (Zeiss Stemi SV 11). Both present good sphericity and low presence of cracks and deformations.

The X-ray diffractograms of the microspheres indicate that the material presented in Figure 4 exhibits low crystallinity, being alumina in one of its transition phases, possibly the gamma phase (γ-Al_2O_3), in accordance with the Joint Committee on Powder Diffraction Standards (JCPDS) 29-0063 [30,31]. Doping with Si was not enough to detect the presence of another crystalline phase.

Table 1 presents the values of specific surface area, volume, and mean pore diameter for pure alumina-based and Si-doped microspheres. Pure microspheres calcined at 700 °C showed a higher specific surface area, reaching 239.03 m^2/g. On the other hand, doping with Si under the conditions employed, caused a reduction in the specific surface, volume, and average diameter of pores.

Figure 5 shows the adsorption/desorption curves of the microspheres produced, determined by the ASAP 2010 specific surface and porosity analyzer, from Micromeritics Corp. The characteristics of the adsorption/desorption isotherm determine the type and size of pores in the sample, thus different forms of hysteresis correspond to types of porosity geometry. In this case, the isotherm format shown in Figure 5 corresponds to materials with regular pores, cylindrical and/or polyhedral with open ends, and may be of the meso and macro pore type [32,33].

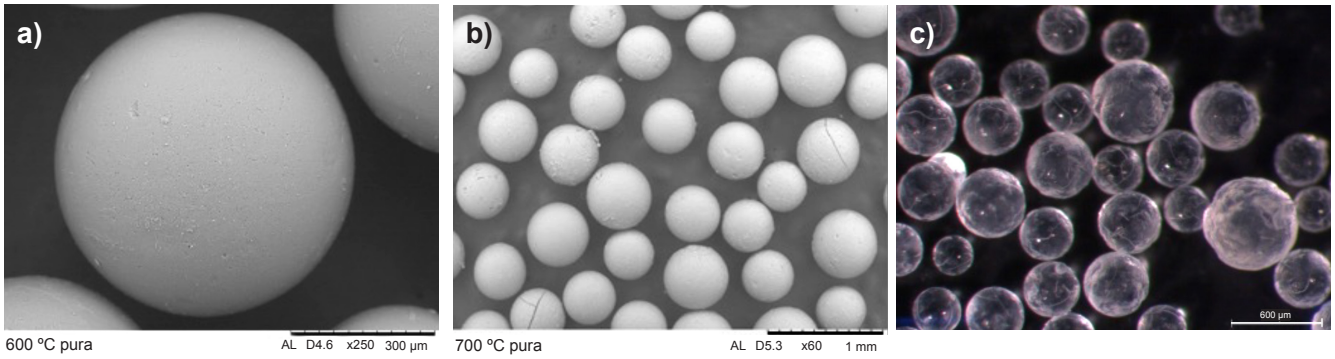

Figure 3: Alumina-based ceramic microspheres.

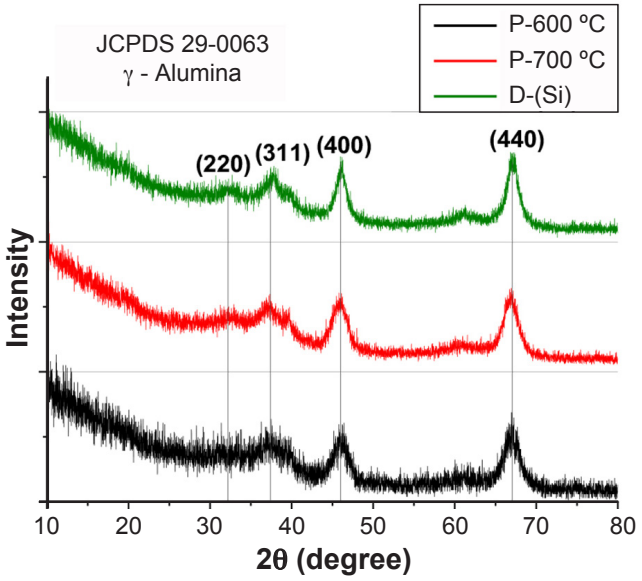

Figure 4 : X-ray diffractograms of microspheres calcined at 600 ºC, microspheres calcined at 700 ºC, and Si-doped microspheres calcined at 700 ºC.

Fixed bed column system

The adsorption process of Zn^{2+}, Ni^{2+}, and Mn^{2+} was carried out by passing the tricationic solution through a fixed-bed column filled with adsorbent microspheres, as shown in Figure 2. The tests lasted about 3 hours each, with the solution flowing through the column at a flow rate of 10 mL/minute, collecting 10 mL quotas of the treated solution every 15 minutes. This liquid was characterized using Inductively Coupled Plasma Optical Emission Spectroscopy (ICP-OES) with the Spectro spectrometer, model ARCOS (Spectro Analytical Instruments Co., Kleve, Germany).

Figure 6 shows the results of the concentration data for each of the heavy metal ions evaluated as a function of time. For all graphs on the zero line of the abscissas, we have the initial concentration of the ion in the solution. It is observed that for each of the tests, varying the microsphere, the initial concentration of heavy metals changed. The figure also indicates, by the dashed line, the maximum permitted concentration of these heavy metals in effluents that can be discarded, established through Resolution Nº 430 of 2011 of the National Council for the Environment (CONAMA). This resolution establishes maximum permitted concentrations of 5.0 $mg.L^{-1}$ zinc, 2.0 $mg.L^{-1}$ of nickel, and 1.0 $mg.L^{-1}$of manganese.

It is observed that for all tests there is a significant

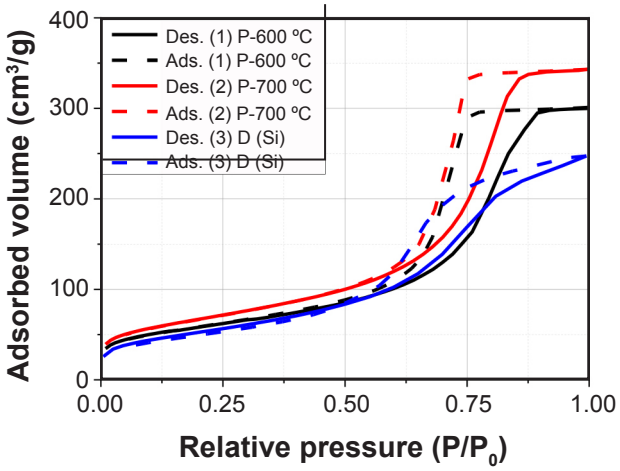

Figure 5: Gas adsorption (BJH) graphs of pure and Si-doped alumina microspheres.

Table I - Specific surface area and porosity of the evaluated microspheres.

Sample	Specific surface (m^2/g)	Pore volume (cm^3/g)	Average pore diameter (Å)
Alumina P-600 °C (1)	210,07	0,47	67,65
Alumina P-700 °C (2)	239,03	0,53	67,77
Alumina D(Si) (3)	191,41	0,39	59,22

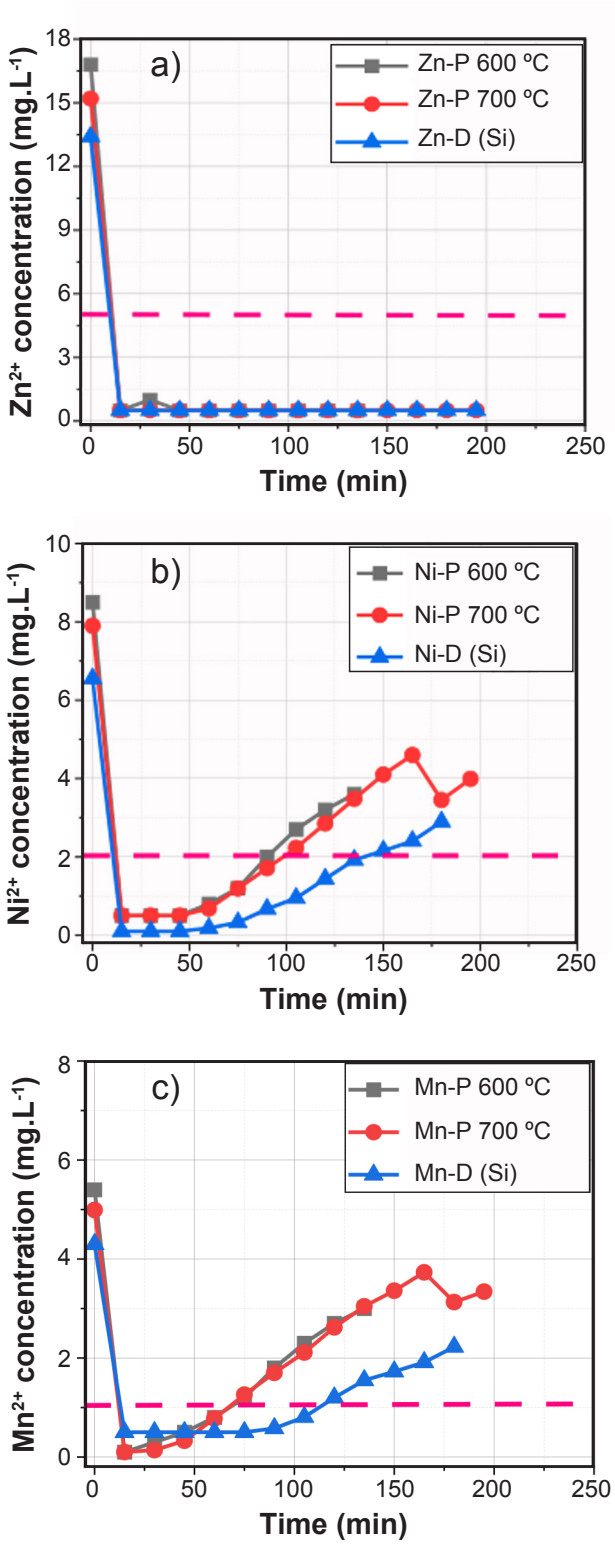

Figure 6: Concentration of heavy metal ions after treatment: zinc (a), nickel (b), manganese (c). The dashed line indicates the maximum concentration of the ion in an effluent allowed by CONAMA.

reduction in the concentration of heavy metals at the beginning of the test, reaching levels below the maximum acceptable. Analyzing the adsorption behavior for each ion separately, it can be seen that for Zn^{2+}, figure 6(a), alumina proved to be a very efficient adsorbent throughout the entire

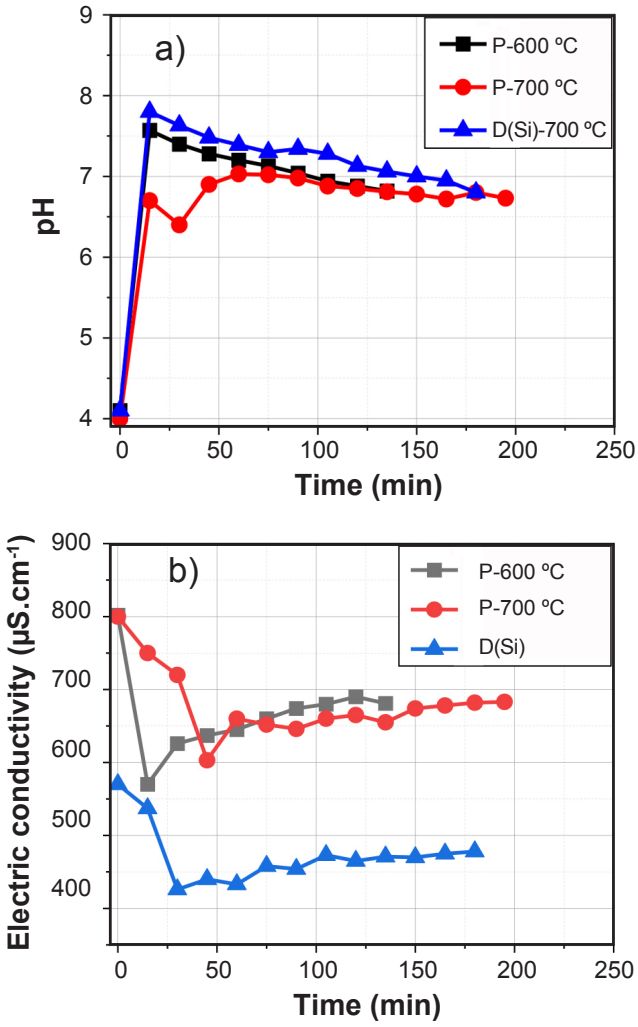

Figure 7: pH (a) and conductivity (b) values of the tricationic solution after treatment.

test. Even after 3 hours of passage of the solution through the column, the Zn^{2+} concentration remained very low, around 0.5 $mg.L^{-1}$. In the case of Ni^{2+} and Mn^{2+} (Figures 6(b) and 6(c), respectively) the observed behavior was different. In Ni^{2+}, with the configuration and conditions used, after 90 minutes of testing, the solution already presents levels above acceptable; the same occurs for Mn^{2+} after 60 minutes of testing. It can therefore be considered that after this volume of treated solution, the microspheres began to reach a saturation of their sites occupied by the ions, however, in the time tested it was not possible to determine the equilibrium.

Under the conditions in which these tests were carried out, therefore, it is possible to state that the microspheres showed a high adsorption capacity for heavy metals, reaching, for the three analyzed ions, a reduction of more than 90% of their initial concentration. However, the challenge is to increase this adsorption capacity.

In this same test, the pH values and electrical conductivity of each sample collected were evaluated, in Figure 7 the results are presented. In the graph of image 7(a), both the initial pH values and those over time are displayed.

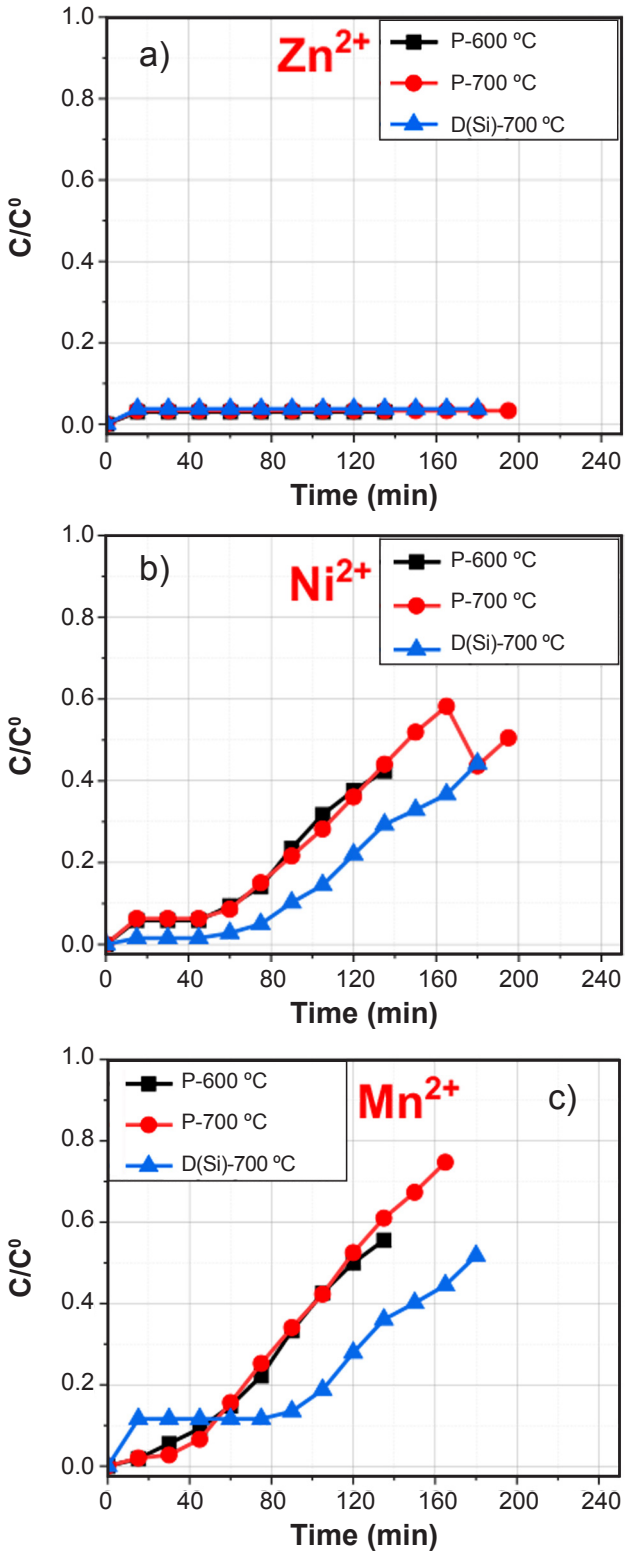

Figure 8: Rupture curves established for Zn^{2+}, Ni^{2+}, and Mn^{2+} for the three types of alumina microspheres studied.

An initial pH of 4 was established, a value that favors the physical and chemical processes of adsorption. In the graph of image 7(b), the conductivity values are presented. The data obtained are in line with expectations, that is, with the evolution of adsorption there is a reduction in electrical conductivity and an increase in pH, also consistent with the observed reduction in ion concentration.

One way to evaluate the performance of the system in fixed-bed columns is through the analysis of the rupture curve. This study describes the dynamic behavior and efficiency of a column, according to the parameters of effluent concentration versus time or volume of treated liquid. The adsorption in the column takes place in the so-called Mass Transfer Zone (MTZ), located where the adsorbate concentration varies from 90% to 5% of the initial value. In this way, it advances between the location of the column that is saturated and the one that still contains free adsorbent. For the MTZ to establish itself, it may take some time, as there is resistance to mass transfer, due to the liquid film around the particle [13,29,34].

In this study, the rupture curves are presented in Figure 8, it is possible to determine the rupture point only for nickel 8(b) and manganese 8(c), which are established by the maximum concentration allowed in the current legislation, that is, C/C_0 by approximately 0.1 in both. However, the exhaustion point could not be determined, since the adsorbent did not reach equilibrium. Thus, the established time was not enough for the alumina microspheres to reach complete saturation to reach equilibrium. In the case of zinc 8(a), after initial adsorption, it remained stable. Likely, the saturation of the adsorbent sites was not sufficient to determine the breaking point.

CONCLUSION

The alumina microspheres produced by the internal gelation method proved to be suitable and efficient as adsorbents for heavy metal ions present in the effluents originating from the tricationic phosphatization process. The calcination temperature, under the evaluated conditions, did not promote significant changes in the alumina adsorption capacity for the analyzed heavy metals. However,over 90% adsorption of adsorption of these heavy metals was obtained, in the fixed-bed column regime, indicating high efficiency of alumina microspheres as adsorbents of Zn^{2+}, Ni^{2+}, and Mn^{2+}. Thus, the microspheres produced by internal gelation, due to their high adsorption capacity, should be considered as an alternative for industrial processes that require treatment for the removal of heavy metals in effluents.

ACKNOWLEDGMENTS

The authors of this research are grateful for the financial support granted by the National Council for Scientific and Technological Development (CNPq), the University of São Paulo (USP), and the Institute of Energy and Nuclear Research (IPEN).

REFERENCES

[1] Sankara Narayanan TSN. Surface pretreatment by phosphate conversion coatings—A review. *Rev Adv Mater Sci*. 2005;**9**:130-77. doi:10.1515/corrrev.1994.12.3-4.201.

[2] Bagal NS, Kathavate VS, Deshpande PP. Nano-TiO2 phosphate conversion coatings—A chemical approach. *Electrochem Energy Technol*. 2018;**4**(1):47-54. doi:10.1515/eetech-2018-0006.
[3] Ezekiel SN, Ayoola AA, Durodola B, Odunlami OA, Olawepo AV. Data on zinc phosphating of mild steel and its behaviour. *Chem Data Coll*. 2022;**38**:100838. doi:10.1016/j.cdc.2022.100838.
[4] Nguyen TL, Cheng TC, Yang JY, Pan CJ, Lin TH. A zinc–manganese composite phosphate conversion coating for corrosion protection of AZ91D alloy: Growth and characteristics. *J Mater Res Technol*. 2022;**19**:2965-80. doi:10.1016/j.jmrt.2022.06.079.
[5] Riyas AH, Geethanjali CV, Arathy S, Anil A, Shibli SMA. Exploration and tuning of Al2O3/Mo composite for enhancement of anti-corrosion and tribological characteristics in zinc phosphate conversion coatings. *Appl Surf Sci*. 2022;**593**:153370. doi:10.1016/j.apsusc.2022.153370.
[6] Milošev I, Frankel GS. Conversion coatings based on zirconium and/or titanium. *J Electrochem Soc*. 2018;**165**(3). doi:10.1149/2.0371803jes.
[7] Ashraf S, Rizvi NB, Rasool A, Mahmud T, Huang GG, Zulfajri M. Evaluation of heavy metal ions in the groundwater samples from selected automobile workshop areas in northern Pakistan. *Groundw Sustain Dev*. 2020;**11**. doi:10.1016/j.gsd.2020.100428.
[8] Briffa J, Sinagra E, Blundell R. Heavy metal pollution in the environment and their toxicological effects on humans. *Heliyon*. 2020;**6**(9). doi:10.1016/j.heliyon.2020.e04691.
[9] Mitra S, Chakraborty AJ, Tareq AM, Emran TB, Nainu F, Khusro A, et al. Impact of heavy metals on the environment and human health: Novel therapeutic insights to counter the toxicity. *J King Saud Univ Sci*. 2022;**34**(3):101865. doi:10.1016/j.jksus.2022.101865.
[10] Innocenzi V, Cantarini F, Amato A, Morico B, Ippolito NM, Beolchini F, et al. Case study on technical feasibility of galvanic wastewater treatment plant based on life cycle assessment and costing approach. *J Environ Chem Eng*. 2020;**8**(6):104535. doi:10.1016/j.jece.2020.104535.
[11] Renu, Agarwal M, Singh K. Heavy metal removal from wastewater using various adsorbents: A review. *J Water Reuse Desalination*. 2017;**7**(4):387-419. doi:10.2166/wrd.2016.104.
[12] Rashid R, Shafiq I, Akhter P, Iqbal MJ, Hussain M. A state-of-the-art review on wastewater treatment techniques: The effectiveness of adsorption method. *Environ Sci Pollut Res Int*. 2021;**28**:9050-66. doi:10.1007/s11356-021-12395-x.
[13] Nascimento RFD, Lima ACA, Vidal CB, Melo DQ, Raulino GSC. Adsorção: Aspectos teóricos e aplicações ambientais. UFC; 2020. doi:10.11606/d.76.2024.tde-20092024-093246.
[14] Chen X, Hossain MF, Duan C, Lu J, Tsang YF, Islam MS, Zhou Y. Isotherm models for adsorption of heavy metals from water—A review. *Chemosphere*. 2022;**307**:135545. doi:10.1016/j.chemosphere.2022.135545.
[15] Rajendran S, Priya AK, Kumar PS, Hoang TK, Sekar K, Chong KY, et al. A critical and recent developments on adsorption technique for removal of heavy metals from wastewater—A review. *Chemosphere*. 2022;**303**:135146. doi:10.1016/j.chemosphere.2022.135146.
[16] Mustapha S, Shuaib DT, Ndamitso MM, Etsuyankpa MB, Sumaila A, Mohammed UM, et al. Adsorption isotherm, kinetic and thermodynamic studies for the removal of Pb(II), Cd(II), Zn(II) and Cu(II) ions from aqueous solutions using Albizia lebbeck pods. *Appl Water Sci*. 2019;**9**:1-11. doi:10.1007/s13201-019-1021-x.
[17] Velarde L, Nabavi MS, Escalera E, Antti ML, Akhtar F. Adsorption of heavy metals on natural zeolites: A review. *Chemosphere*. 2023;**328**:138508. doi:10.1016/j.chemosphere.2023.138508.
[18] Busca G. The surface of transitional aluminas: A critical review. *Catal Today*. 2014;**226**:2-13. doi:10.1016/j.cattod.2013.08.003.
[19] Busca G. Silica-alumina catalytic materials: A critical review. *Catal Today*. 2020;**357**:621-29. doi:10.1016/j.cattod.2019.05.011.
[20] Rahmani A, Mousavi HZ, Fazli M. Effect of nanostructure alumina on adsorption of heavy metals. *Desalination*. 2010;**253**(1-3):94-100. doi:10.1016/j.desal.2009.11.027.
[21] Rajabzadeh M, Aghaie H, Bahrami H. Thermodynamic study of Iron (III) removing by the synthesized α-Alumina powder and evaluating the corresponding adsorption isotherm models using Response Surface Method. *Arab J Chem*. 2020;**13**(2):4254-62. doi:10.1016/j.arabjc.2019.07.006.
[22] Mahesh R, Vora K, Hanumanthaiah M, Shroff A, Kulkarni P, Makuteswaran S, et al. Removal of pollutants from wastewater using alumina based nanomaterials: A review. *Korean J Chem Eng*. 2023;**40**(9):2035-45. doi:10.1007/s11814-023-1419-x.
[23] Guo F, Wu F, Li J, Liu L, Huang Y. A facile approach for preparing Al2O3 reticulated porous ceramics with optimized closed-cell struts and excellent mechanical properties. *Ceram Int*. 2023;**49**(13):22054-61. doi:10.1016/j.ceramint.2023.04.031.
[24] Wang L, Liu J, Rong Y, Yan S, Yu M, Li X, et al. Novel design of microsphere adsorbent for efficient heavy metals adsorption. *Int J Appl Ceram Technol*. 2020;**17**(5):2228-39. doi:10.1111/ijac.13538.
[25] Moreira TM, Genova LA. Influência da composição e distribuição de tamanho de microesferas de Al2O3/Fe2O3, produzidas por gelificação interna, na adsorção de metais pesados. *Matéria (Rio J)*. 2023;**28**(2). doi:10.1590/1517-7076-rmat-2023-0004.
[26] Colak G, Leinders G, Delville R, Jutier F, Verwerft M, Vleugels J. Infiltration of porous uranium oxide microspheres prepared by internal gelation. *J Nucl Mater*. 2022;**562**:153587. doi:10.1016/j.jnucmat.2022.153587.
[27] Ding X, Ma J, Zhao X, Hao S, Li Z, Deng C, Li G. Preparation of CeO2 microspheres by internal gelation process with copolymerization using acrylic acid. *Ceram Int*. 2019;**45**(9):11571-77. doi:10.1016/j.ceramint.2019.03.027.
[28] Danish M, Ansari KB, Danish M, Khatoon A, Rao RAK, Zaidi S, Aftab RA. A comprehensive investigation of external mass transfer and intraparticle diffusion for batch and continuous adsorption of heavy metals using pore volume and surface diffusion model. *Sep Purif Technol*. 2022;**292**:120996. doi:10.1016/j.seppur.2022.120996.
[29] da Silva Neto HA, Garcia HL, Araujo RGO, Garcia CAB. Adsorção em coluna de leito fixo aplicada para a pré-concentração de cádmio em amostras de água. *Scientia Plena*. 2018;**14**(6). doi:10.14808/sci.plena.2018.064208.
[30] Moghadam TM, Alizadeh P, Ghamari M, Mousavi M. A green chemical approach for synthesis of sponge-like mesoporous gamma alumina and evaluation of three

parameters OH/Al, salt concentration and ageing time on BET and BJH properties. *Int Nano Lett*. 2021;**11**(2):141-47. doi:10.1007/s40089-021-00327-z.
[31] Su J, Liu Y, Peng X, Sun G, Jiang X. Synthesis of α-Al2O3 nanoparticles with uniform size distribution by stearic acid-assisted mechanochemical method. *Powder Technol*. 2024;**437**:119529. doi:10.1016/j.powtec.2024.119529.
[32] Sing KS. Reporting physisorption data for gas/solid systems with special reference to the determination of surface area and porosity (Recommendations 1984). *Pure Appl Chem*. 1985;**57**(4):603-19. doi:10.1351/pac198557040603.
[33] Schlumberger C, Thommes M. Characterization of hierarchically ordered porous materials by physisorption and mercury porosimetry—A tutorial review. *Adv Mater Interfaces*. 2021;**8**(4):2002181. doi:10.1002/admi.202002181.
[34] Salehi E, Askari M, Darvishi Y. Novel combinatorial extensions to breakthrough curve modeling of an adsorption column—Depth filtration hybrid process. *J Ind Eng Chem*. 2020;**86**:232-43. doi:10.1016/j.jiec.2020.03.015.
(Rec. 02-Feb-2024, Rev. 14-Mar-2024, Rev. 17-Apr-2024, Ac. 19-May-2024)
(AE: Daniel Z. de Florio)